Russian Geology and Geophysics
Vol. 38, No. 1, pp. 82-96, 1997

Geologiya i Geofizika
UDC 552.348.550.4

THE MERLIN KIMBERLITES, NORTHERN TERRITORY, AUSTRALIA

D. C. Lee, H. J. Milledge*, T. H. Reddicliffe, B. H. Scott Smith**, W. R. Taylor*, and L. M. Ward

Ashton Mining Limited, 21 Wynyard Street, Belmont, Western Australia 6104, Australia
**Department of Geological Sciences, University College, Gower Street, London, United Kingdom*
***Scott-Smith Petrology, 2555 Edgemont Boulevard, North Vancouver, BC VR7 2M9, Canada*

The Merlin kimberlites are located in the Batten region of the Northern Territory of Australia, 800 km southeast of Darwin. The kimberlites are in a 10 km by 5 km field on the eastern side of the Batten Trough and occur in four clusters. None outcrop but eleven have been found and it is probable that more remain to be discovered.

Two generations of pseudomorphed olivine are present and the nature of the olivines, the matrix and the complex texture of the rocks are all typical of kimberlites. Well-developed pelletal textures and the presence of xenolithic material show that some of the rocks are diatreme-facies but a few samples have uniform groundmasses and appear to be hypabyssal kimberlite.

Extensive alteration and the presence of xenoliths has affected the geochemistry of most samples but the rocks are ultrapotassic (molar K/Na > 2) with a low TiO_2/K_2O ratio, similar to micaceous kimberlites and some phlogopite lamprophyres. The ratios Ni/MgO and FeO_t/MgO are within the normal range of kimberlites and olivine lamproites. Nb/Zr is exceptionally high. Macrocrysts include chrome-spinel, periodotitc garnets and chrome diopside. Megacrysts are absent.

Diamonds occur in all eleven kimberlites. Infra-red spectra of microdiamonds indicate that there are three main time-temperature populations present and the size distribution and range of morphologies also suggests several populations. Exceptionally high levels of hydrogen are indicated by infra-red spectra for some of the diamonds.

Kimberlites, Australia, diamonds, chrome spinels, pyrope garnets

INTRODUCTION

The Merlin field of kimberlites was found in 1993 and 1994 by intensive exploration work in the Batten region of the Northern Territory. Eleven kimberlites, named Excalibur, Palomides, Sacramore, Launfal, Kay, Ywain, Gawain, Tristram, Garath, Ector and Bedevere, occur in four clusters within a 10 km by 5 km oblate field. The kimberlites are small, the largest being 125 m in diameter. Drilling has shown that the kimberlites have an almost constant diameter to a depth exceeding 100 m.

REGIONAL GEOLOGY

The Batten region is situated on the eastern side of the North Australian Craton (Fig. 1). The area south of the western edge of the Gulf of Carpentaria is dominated by the Middle Proterozoic McArthur Basin which extends over an area of 180,000 km^2 [1] and forms part of the North Australian Platform. Early Proterozoic basement rocks include the Scrutton Volcanics which have been dated by U-Pb in zircon at 1857±30 Ma. Cambrian age Bukalara sandstone, 30 to 100 m thick, overlies the McArthur Basin in much of the region and frequently forms plateaux.

Cretaceous sedimentation has been widespread in the area but it is now largely removed for a distance of 200 km south from the Gulf of Carpentaria coastline. The southern limit of the stripping is marked by a

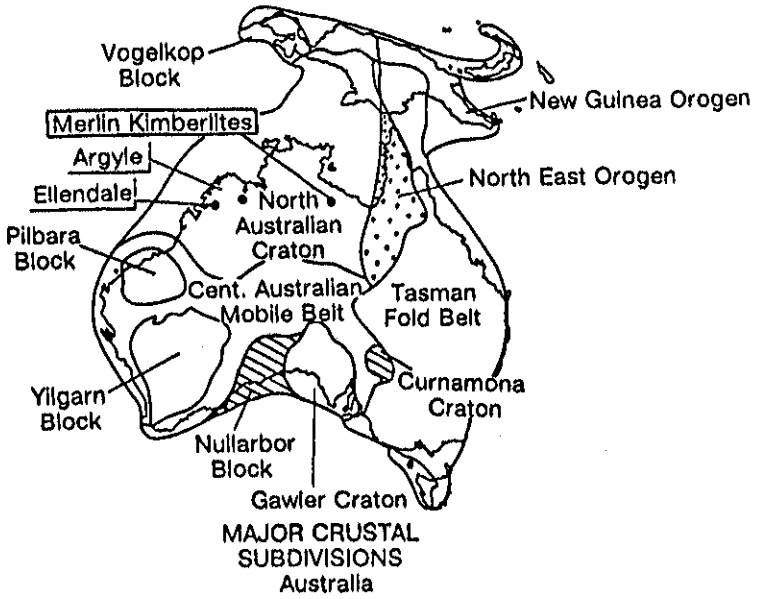

Fig. 1.

well defined escarpment which acts as a drainage divide. Streams to the south flow southwards, while those on the north side of the scarp flow north to the Gulf of Carpentaria.

The major structural feature of the southern McArthur Basin is the Batten Trough, also known as the Batten Fault Zone. The Batten Trough, bounded on the east by the Emu Fault and obscured to the west by the Roper Group of sedimentary rocks, is a synsedimentary graben containing up to 10 km of McArthur Basin sediments. The trough is a 70 km wide zone of extensive faulting, trending north northwest. The Merlin kimberlite field is intruded to the east of the southern end of the Batten Trough between two major faults, the Emu Fault and the Calvert Fault.

GEOLOGY OF THE KIMBERLITE FIELD

The eleven kimberlite pipes and associated dykes are intruded through Bukalara sandstone. Surface expression is almost entirely absent as the pipes are covered by locally derived broken sandstone blocks and sediments. In a few instances, a shallow depression can be seen at the surface but there is an abundance of similar depressions in the surrounding countryside which are not associated with kimberlites.

Four clusters of kimberlites have been located in the field which is 10 km long by 5 km wide. Within the clusters, the pipes are sometimes very closely spaced, being 100 to 200 m apart. The pipes are steep sided and almost cylindrical in shape. Concentric fracturing in the Bukalara sandstone surrounds the pipes.

Some small brecciated zones of sandstone occur along narrow kimberlite dykes which extend outside of the main field of kimberlites. More extensive brecciated zones of Bukalara sandstone occur adjacent to one cluster of kimberlites. The brecciation is thought to have been caused by the emplacement of small dykes or by explosive volcanism associated with the kimberlites as the brecciated zones are enriched in Ce, La and Nb and contain small diamonds and kimberlitic chrome spinels.

Drill core shows that the kimberlites are overlain by a sequence of mudstones and fine to medium grained sandstones, typically 20 m thick. Immediately above the kimberlite is a one metre thick layer of quartzite boulders. Drill core samples from the kimberlites show that there is variation in texture, xenolith content and the degree of weathering but most samples are typical of diatreme facies kimberlites. Some samples from a depth of approximately 100 m in the Launfal pipe appear to be hypabyssal kimberlite but other samples from a similar depth have the characteristics of diatreme facies kimberlite. Further drilling and sampling is necessary before a complete description of the structure of the Merlin kimberlites can be given. An emplacement age of 367±4 Ma has been determined from a single sample of drill core by Rb-Sr in mica age dating techniques.

PETROGRAPHY

The rocks are difficult to investigate petrographically because of the extensive alteration which includes carbonatisation, silicification, partial replacement by secondary sulphides, clay mineralisation and chloritisation. The samples examined for this study were limited to three pieces of drillcore from three bodies and five composite drillchip samples from five bodies. A total of seven bodies were examined. The drillcore samples derive from depths between 30–232.5 m while the drillchips derive from between 70 and 103 m.

All the rocks contain two generations of pseudomorphed olivine which include anhedral and often rounded macrocrysts (up to 15 mm) as well as numerous smaller (<1 mm) typically euhedral phenocrysts. Mica phenocrysts (up to 1 mm) are present in variable abundances. The mica occurs as lath-like grains which are typically partially altered to green chlorite and distorted by the secondary replacement processes. At Excalibur, some of the mica phenocrysts were formed by two phases of crystallisation. Some of the earlier clear cores have been overgrown by a late stage mica which poikilitically encloses fine grained spinel grains similar to those that occur in the adjacent groundmass. The two phases of mica have slightly different optical properties and probably have different compositions. The interstitial areas between the constituents described so far often appear to be poorly crystalline. In most instances this feature, together with the alteration, make strict rock type [after 2–4] and mineralogical [after 5] classifications difficult. Observed primary groundmass minerals include mica, spinel, apatite, serpentine and carbonate (the latter at Ector, Excalibur and Palomides). Possible groundmass monticellite pseudomorphs were observed at Kay and Ector. The nature of the olivines and the mineralogy of the matrix is typical, or even diagnostic, of kimberlites and are not characteristic of other rock types such as lamproites. This feature strongly supports the classification of these rocks as kimberlites. Further support comes from the presence of significant quantities of diamond as well as mantle-derived spinel, garnet and chrome diopside. Importantly, no features were observed which suggest that these rocks are not kimberlites. Even though mica is common and ilmenite rare or absent, the nature of the mica and the presence of abundant groundmass spinel and possible monticellite suggest that the kimberlites are similar to Group 1 kimberlites.

Varied abundances and types of xenoliths are present in the drillcore samples. Extraneous material is also common among the drill chips.The presence of occasional kimberlite skins on the extraneous fragments indicates that some of the fragments were resident in the kimberlite. Some samples contain sufficient xenolithic material to be classified as kimberlite breccias. The xenolithic material includes carbonates, quartzose rocks and laminated fine grained sediments as well as igneous rocks such as granite and glimmerite. Some of the xenoliths have been "kimberlitised", sometimes beyond recognition [6]. The replacement material is varied and the xenoliths also display zonal alteration.

The textures in the kimberlites are complex, very typical of kimberlites and, as in other kimberlites, difficult to interpret [textures after 7–10]. A few rocks have uniform groundmasses and appear to comprise hypabyssal kimberlites. More common are non-uniform textures. Irregular segregationary groundmasses occur in hypabyssal kimberlites at Excalibur (serpentine with minor carbonate) and Ector (carbonate). Other rocks have well developed pelletal textures (Fig. 2). Most of the pelletal structures comprise a single olivine or mica grain surrounded by a thin rim of very fine grained material. In a few instances probable microlitic textures were observed within the rims. The interclast matrices of these rocks appear to be composed of serpentine with rare microlitic textures while carbonate is absent. These textures are a hallmark of diatreme-facies kimberlites. Such rocks can be described as pelletal tuffisitic kimberlite (breccias). Although difficult to discern, the probable microlites appear to be composed of mica (in Launfal, Gawain and possibly Bevedere). Clinopyroxene is more typical of diatreme-facies kimberlites elsewhere, so this feature seems somewhat unusual. In one sample (from Gawain) pelletal textures are not developed and the rock appears to be composed of single grains of olivine and the rock is classified as a tuffisitic kimberlite breccia. There is no evidence to suggest that any of the samples classified as tuffisitic kimberlites are crater-facies rocks.

At Palomides, in addition to the thin rimmed pelletal lapilli just described, all the rocks examined contain common coarser (up to 10 mm) spherical structures giving the rocks a distinctive appearance (Fig. 3). These structures are composed of a kernel of olivine or a xenolith with a thick (up to at least 5 mm) dark grey kimberlite selvage. Other similar structures may have no apparent kernel. The selvages are composed of olivine phenocrysts, mica, possible primary carbonate laths in a matrix of serpentine and carbonate. The groundmass in the selvages probably crystallised rapidly. The interclast areas are composed of serpentine and variable amounts of carbonate. The paragenesis of carbonate is notoriously difficult to determine and it is not clear if any of the carbonate in these rocks is primary. The larger spherical structures and any primary carbonate, especially in the interclast areas, are more typical of globular segregationary hypabyssal kimberlites while the

Fig. 2. Gawain pipe. The pelletal textures shown here are typical of diatreme-facies kimberlites. The pelletal lapilli are composed of light colored olivine pseudomorphs with groundmass rims that probably have microlitic textures. The interclast matrix is composed of probable serpentine. Field of view is equal to 1.6 mm.

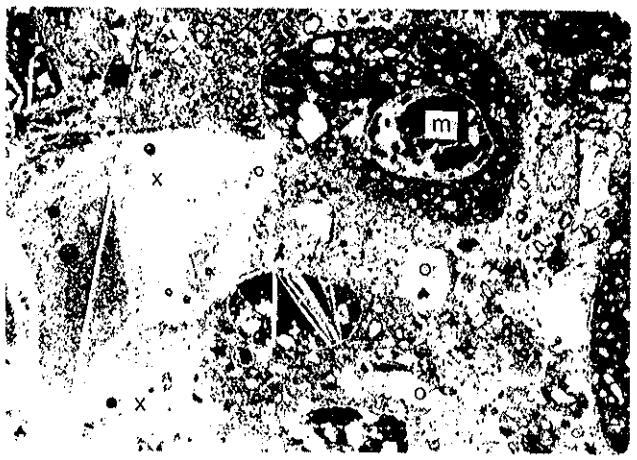

Fig. 3. Palomides pipe. The lapilli-like structures are coarser than that shown in Fig. 2. They are composed of abundant olivines (o), a carbonised xenolith (x) and dark groundmass. The latter contains common fine laths of carbonate. The olivines include both anhedral macrocrysts (m) and more common smaller phenocrysts. The olivines have been pseudomorphed by light colored serpentine (o) or carbonate and a few macrocrysts (m); some dark secondary material is also present. The interclast matrix is composed of a mixture of carbonate and serpentine. Field of view is equal to 10 mm.

smaller pelletal lapilli are more typical of diatreme-facies kimberlites. It is possible that the larger structures formed either (i) during diatreme formation or (ii) earlier during ascent in a more hypabyssal-like environment and then were carried through into the final fluidisation process during diatreme formation.

A sample from Kay is composed of more uniform fragments of kimberlite set in a carbonate-rich matrix. None of the features typical of diatreme-facies rocks are present in this sample but there is insufficient evidence

to determine whether the sample derives from the hypabyssal or crater-facies. Given the nature of the other samples from this province, the latter option seems unlikely.

The classifications of the samples are given by occurrence below:

Bedevere:	Possible diatreme-facies kimberlite (rather than hypabyssal).
Ector:	Hypabyssal macrocrystic kimberlite with a segregationary groundmass.
Excalibur:	Altered probable hypabyssal mica-bearing kimberlite, and a relatively fresh hypabyssal macrocrystic segregationary serpentine phlogopite kimberlite (this sample shows similarity to the hypabyssal kimberlite from Launfal).
Gawain:	Tuffisitic pelletal kimberlite (breccia) and tuffisitic kimberlite breccia, both of the diatreme-facies.
Kay:	Serpentine phlogopite kimberlite which may be derived either from the hypabyssal or crater-facies (former considered more likely).
Launfal:	Hypabyssal spinel-bearing mica kimberlite (with somewhat unusual features) and probable pelletal tuffisitic kimberlite breccia of the diatreme-facies.
Palomides:	Probable diatreme-facies pelletal tuffisitic kimberlite (breccia).

ANALYTICAL METHODS

Geochemistry. Whole-rock geochemistry results were obtained by Analabs Pty Ltd, Perth. Major elements were analysed by glass fusion XRF, Zu, Zn, Ga, Rb, Sr, Y, Pb, Ba, La, Ce and Th by ICPMS, Ni by AAS and V, Cr, Zr and Nb by pressed powder XRF. FeO was determined by titration methods and LOI and H_2O by gravimetric methods.

Mineral analyses were determined at the Electron Microscopy Centre, University of Western Australia. Major and minor constituents were determined by EDS analysis using the Centre's JEOL 6400 SEM, fitted with a Link Analytical Si (Li) detector and MCA. The SEM was operated at 15 kV, with a beam current of 3 nA. Each mineral was examined using secondary and backscattered electron imaging to avoid inclusions, exsolution, reacted products and artifacts. Spectra were collected for sixty seconds live time, and intensities of characteristic lines were calculated from these using the "PIBS" technique of Ware, 1981 [11]. Intensities obtained in this way were compared with data from reference standards.

Age dating for a single sample of rock was carried out by AMDEL Limited, of Frewville, South Australia. Standard sample preparation techniques were used to concentrate phlogopite, Rb and Sr concentrations and the Sr isotopic ratios were determined using a Finnigan MAT261 mass spectrometer.

Infra-red spectra were obtained for some microdiamonds by using a Bruker FT infra-red spectrometer with a Nikon microscope and motorised drive.

Isotopes. Carbon isotopic compositions of the diamonds were measured using sealed tube bulk combusted platinum or quartz buckets, with approximately 5 mg of high purity CuO powder (Specpure, Johnson Mattheu, Royston, England) added prior to evacuation to 10^{-5} millibars or better, inside a 6 mm (id)×4 mm (id) quartz tube. A length of about 5 cm of tube containing the bucket and its contents was then sealed under vacuum with a H_2O_2 flame to give an ampoule of approximately 2 ml volume.

Each specimen was combusted overnight at 1000 °C before cooling to 600 °C for analysis. Carbon dioxide produced was extracted from the ampoule by cracking this inside a vacuum line and purified cryogenically by trapping at –196°C and releasing again at –130 °C. The amount of carbon dioxide was quantified using a capacitance nanometer and the yield checked against the known weight of the starting samples. Any analysis with a yield error greater than ±2% was discarded. The CO_2 was then isotopically measured on a SIRA 24 mass spectrometer against a working standard prior to calculation of the results to the PDB scale. Isotopic data obtained are subject to errors of less than ±0.05%.

GEOCHEMISTRY

Extensive alteration of the kimberlites and contamination by xenoliths has affected the geochemistry of most samples. One sample of carbonatised rock from Palomides and a drillcore sample from a depth of 248 m in Excalibur have a low ilmenite index <47 [Ilmenite Index = $(FeO_t + TiO_2)/(2\ K_2O + MgO)$] that falls within the range of relatively unaltered kimberlite [12]. The trace element ratios of these samples should, therefore, provide a reasonable basis for comparison with other kimberlites so that the geochemical affinities of the Merlin kimberlites can be established.

Table 1

Comparison of Key Geochemical Ratios for the Merlin Rocks and Average Kimberlite/Related Rocks

Ratio	Merlin		Aries kimberlite	Bow Hill Lampro-phyre	Koidu kimberlite	Group I kimberlite	Group II kimberlite	Olivine kimberlite
	Palomides	Excalibur						
FeO_t/MgO	0.43	0.36	0.40	0.36	0.34	0.32	0.30	0.33
Ni/MgO	39	41	61	48	42	40	49	34
TiO_2/K_2O	0.28	0.16	0.48	0.22	1.27	1.70	0.42	0.84
K/Na*	5	52	3	5	9	2	10	6
$(P_2O_5/Ce)\cdot 10^4$	20	16	9	13	18	58	33	34
Nb/Zr	3.7	3.5	4.2	0.9	1.7	1.1	0.48	0.2
Ba/Rb	17	9	12	9	24	26	19	20
Nb/La	1.3	0.7	1.7	1.3	1.4	1.8	0.7	0.8

Note. Global kimberlite and related rock averages are from Taylor et al. [12].
***Molar ratio.**

Table 1 lists the key geochemical ratios for the Merlin kimberlite sample and the ratios for average samples of kimberlites and related rocks elsewhere. The Merlin rocks have an ultrapotassic composition (molar K/Na >2) with a low TiO_2/K_2O ratio similar to micaceous kimberlites and some phlogopite lamprophyres such as that from Bow Hill [13]. The Ni/MgO and FeO_t/MgO ratios are within the range of kimberlites and olivine lamproites, indicating that the rocks are derived from a primitive mantle source. The P_2O_5/Ce ratio for the least altered samples is lower than that of South African Group I or II kimberlites but similar to that of the Koidu and Aries kimberlites (Fig. 4).

A useful geochemical indicator is the Nb/Zr ratio because Nb and Zr are not strongly susceptible to alteration and these elements tend to be diagnostic of a particular mantle source. For the Merlin kimberlites, Nb/Zr is very high (Table 2), having a value close to that of the Aries kimberlite (Fig. 4). The high Nb/Zr ratio clearly indicates that the Merlin kimberlites do not have geochemical affinities with olivine lamproites

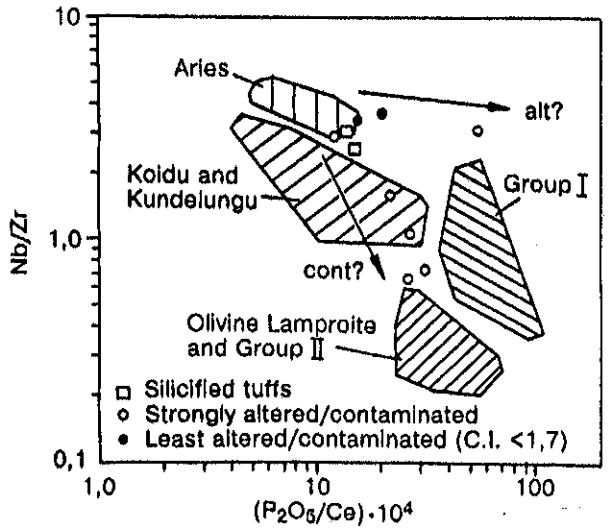

Fig. 4. Discriminant plot based on trace element ratios that have strong source-diagnostic characteristics. Field plotted from the kimberlite/lamproitic database KIMDAT [12] to cover >90% of the data points for each chemically distinct kimberlite/lamproite group. The least altered Merlin kimberlites (contamination indices <1.7) are most closely allied to the Aries kimberlite. A probable alteration-only trend (alt?) toward higher P_2O_5/Ce, and a crustal contamination plus alteration trend (cont?) toward higher P_2O_5/Ce plus lower Nb/Zr are indicated by arrows.

Table 2

Merlin Kimberlite (Least Altered)

Component	Palomides	Excalibur
	Carbonatised olivine-mica rock	Olivine-mica volcanic rock
	Sample No. BB130 (depth 71.72 m)	Sample No. BB113 (depth 248.10 m)
SiO_2	28.00	30.10
TiO_2	0.45	0.52
Al_2O_3	3.64	4.30
FeO_t	7.86	8.10
MnO	0.10	0.15
MgO	16.56	20.30
CaO	20.43	13.90
Na_2O	0.19	0.04
K_2O	1.58	3.17
P_2O_5	0.49	0.51
LOI	19.38	18.18
Total	98.68	99.27
C. I.	1.61	1.29
Ilm. I.	0.38	0.29
Trace elements (ppm)		
Sc	–	12
V	59	80
Cr	938	1200
Ni	644	842
Co	–	66
Zn	137	50
Rb	174	310
Sr	1250	1100
Y	10	11
Zr	64	55
Nb	238	190
Pb	4	–
Ba	2950	2660
La	181	260
Ce	241	330
Th	51	–

(such as Argyle) or Group II kimberlites. Other ratios such as low Ba/Rb and high Nb/La are also characteristic of an Aries signature.

In conclusion, the Merlin kimberlite have geochemical features that indicate they are allied with the Aries kimberlite and Bow Hill lamprophyres in the Kimberley region of Western Australia. The kimberlites were evidently generated from a geochemically anomalous deep mantle source that underlies parts of the North-Australian Craton.

MINERAL CHEMISTRY

A large proportion of the minerals originally present in the kimberlites has been destroyed by alteration and can now only be seen as pseudomorphs in polished thin sections. Samples of rock extracted by Rotary-Air-Blast drilling were processed to extract mineral concentrates which contain chrome spinel, garnet, chrome-rich clinopyroxene, apatite and sulphide. Minor amounts of galena, sphalerite, iron sulphides and zircon, probably derived from local crustal rocks, are also present.

Chrome spinels. Chrome spinels dominate the mineral assemblage. They are common in all Merlin kimberlites with the exception of Bedevere which has only a few macrocrysts. Representative major element analyses for the spinels are presented in Table 3. The spinels have chrome contents varying from 20 wt.% Cr_2O_3 to 70 wt.% Cr_2O_3 but in most pipes there is a dominant group with chrome content in the range 50 to 65 wt.% Cr_2O_3. A lesser group with 30 to 40 wt.% Cr_2O_3 also occurs.

The morphology of the spinels varies from euhedral to highly irregular and the maximum size is approximately 1 mm. There appears to be no correlation between the morphology and chemistry of the spinels.

Figure 5 illustrates the chrome vs magnesium content of Merlin chrome spinels. Some of the spinels with high chrome content have compositions similar to spinels in diamond bearing xenoliths elsewhere in the world. A few have compositions comparable with diamond inclusion spinels [15].

Garnets. Small quantities of pyrope garnet are present in the Merlin kimberlites. It is believed that most of the garnets have been destroyed by weathering near the surface but they occur frequently in drill core from depths of 50 m or more in some of the pipes. Representative major element analyses are shown in Table 4.

Figure 6 illustrates the range of CaO and Cr_2O_3 in the Merlin garnets. Most are lherzolitic but low calcium, high chrome harzburgitic garnets do occur.

Clinopyroxene. Bright green chrome bearing clinopyroxene, in the form of discrete, rounded grains (0.4 mm), were recovered from Kay and representative major element analyses are listed in Table 3. The clinopyroxenes have low Al_2O_3 (0.86 to 2.16 wt.%) and high chrome content (1.08 to 2.94 wt.%), similar to Cr-rich megacryst clinopyroxenes from kimberlites elsewhere.

Diamonds. All eleven Merlin kimberlites contain diamonds. Ten to twenty tonne samples, extracted by large diameter drilling, have been processed and +1 mm diamonds obtained. One thousand tonne samples from the pipes Palomides and Sacramore have also been processed and suites of diamonds, with a size range from 0.01 carats to in excess of 5 carats (10 mm) were recovered. Further sampling is to be carried out by removal of overburden and trenching. The diamonds have not been systematically described, however, dodecahedra and more extensively resorbed forms are present in approximately equal proportions. A few are unresorbed octahedra and the precentage with visible evidence of plastic deformation is relatively low. Some cube and resorbed cube diamonds occur, mainly in the smaller sizes. The cube forms include some bright yellow diamonds with extensive resorption and etch channels.

Microdiamonds. Microdiamonds (0.1 mm to 0.8 mm) are abundant in the Merlin kimberlites and exceed six per kilogram in some samples. The microdiamonds are predominantly clear, colourless octahedra and macles. In the smaller sizes (<0.2 mm), the proportion of cubes, resorbed cubes and irregular rounded diamonds increases. The irregular rounded microdiamonds are often opaque and poorly crystalline with numerous inclusions and flaws. There is a very large discontinuity in the size distribution at 0.2 mm. For example, of 1,402 microdiamonds extracted from a sample of Merlin kimberlite, 1,194 were >0.1 mm <0.2 mm. The remaining 208 >0.2 mm diamonds are distributed in a more normal way, declining in number with increasing size (Fig. 7).

IR spectra were obtained for 40 microdiamonds from the pipes Excalibur, Palomides and Ywain, and the spectral data for 40 Excalibur microdiamonds is listed in Table 5. The nitrogen content and aggregation state is highly variable. It includes diamonds with less than 250 ppm nitrogen and a very high aggregation state and diamonds with over 1,000 ppm nitrogen and no 1aA/1aB aggregation. The variation in nitrogen content and aggregation state for the diamonds suggests that at least three populations are present. One golden yellow specimen contained a small percentage of nitrogen in the Ib form indicating it represents a very young diamond and/or one that formed under low temperature conditions (<1,000 °C).

Microdiamonds from Palomides have a wide range of nitrogen concentrations, ranging from a few ppm to 2,000 ppm. Three specimens with over 1,500 ppm nitrogen have exceptionally high hydrogen concentrations, while other microdiamonds have none. This suggests at least two populations are present.

The microdiamonds from Ywain also have wide variations in nitrogen and hydrogen contents.

Table 3

SEM-EDS Analyses of Representative Range of Spinels from Merlin Kimberlites

Oxide	1	2	3	4	5
TiO_2	0.16	0.22	0.65	0.29	1.00
Al_2O_3	11.6	3.40	5.37	37.6	12.8
Cr_2O_3	59.0	67.9	62.9	27.2	38.0
Fe_2O_3	1.59	1.53	3.02	3.86	20.1
V_2O_3	0.33	0.22	0.34	0.20	0.13
FeO	14.4	14.2	17.1	18.4	16.4
MnO	0.00	0.00	0.37	0.00	0.29
MgO	12.8	12.1	10.50	12.9	11.7
NiO	0.00	0.00	0.00	0.38	– 0.28
Total	99.8	99.4	99.9	100.3	98.8
Mg#	61.2	60.2	52.2	55.5	56.0

Table 4

SEM-EDS Analyses of Representative Range of Pyrope Garnets and Two Clinopyroxenes

Oxide	1	2	3	4	5	6	7
SiO_2	41.6	40.7	41.4	42.2	42.7	55.8	55.1
TiO_2	0.00	0.00	0.00	0.16	0.00	0.00	0.00
Al_2O_3	16.6	14.5	14.3	21.1	17.3	2.14	0.86
Cr_2O_3	8.54	11.9	10.4	1.88	6.58	2.39	1.51
Fe_2O_3	1.72	0.82	3.13	1.98	3.09	0.68	1.05
FeO	5.49	7.26	4.75	7.79	4.13	1.73	1.46
MnO	0.28	0.38	0.28	0.16	0.00	0.00	0.00
MgO	22.4	18.3	20.4	18.2	21.9	16.8	17.2
CaO	2.61	6.65	5.53	7.20	4.14	18.2	21.1
Na_2O						2.54	1.48
Total	99.27	100.45	99.91	100.55	99.52	100.27	99.84
Mg#	87.9	81.8	88.5	80.65	90.4	94.5	95.4

Note. 1–5 — pyrope garnets; 6 and 7 — chrome clinopyroxenes.

A significant number (50%) of the microdiamonds from Merlin kimberlites are composite stones (twins or aggregates) indicating multiple nucleation and hence a relatively abundant supply of carbon. Twenty percent contain inclusions.

Quantitative analysis of the nitrogen data indicates that there are three main time-temperature populations of microdiamonds (Fig. 8):

(i) a cool and/or young population of mainly pure type IaA stones (nitrogen aggregation temperatures – T(NA) ~1025 °C for 1.65 Ga residence in the mantle);

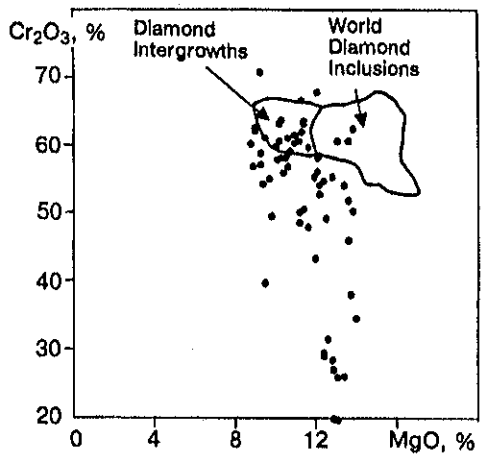

Fig. 5. Merlin chrome spinels (Fields from Smith et al., 1987 [14]).

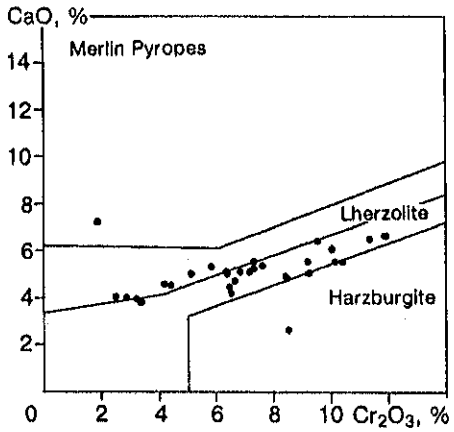

Fig. 6. Merlin garnets (Fields after Sobolev, 1974 [16]).

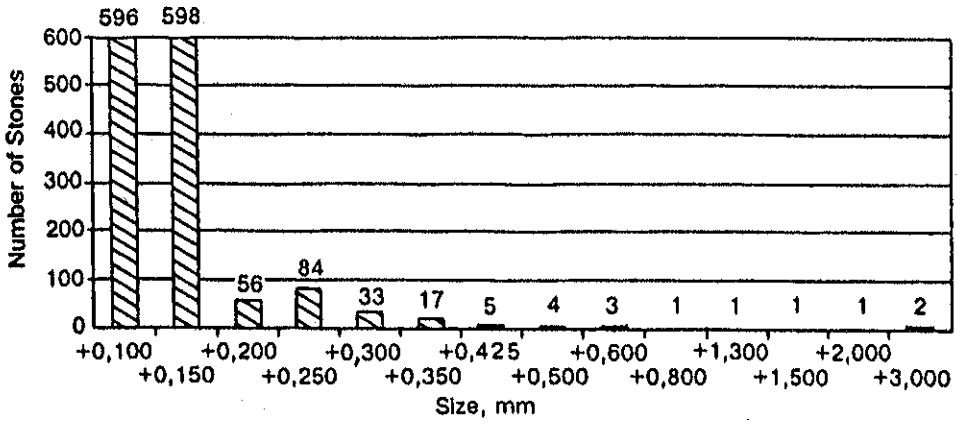

Fig. 7. Size distribution for 1,402 + 0.1 mm diamonds from the Gawain pipe.

(ii) a moderate temperature population of type IaAB diamonds (T(NA) ~1100–1500 °C for a 1.65 Ga residence time) with platelet intensities (type-M behaviour) consistent with these T(NA) values. Some of these diamonds such as EC-08 show strong zonation;

Table 5

Physical Properties and IR Spectral Data for Ector Microdiamonds

Specimen/ Spect. No.	Color	Resorption degree	External form	Birefringence	Inclusions	$\delta^{13}C$, ‰	$\delta^{15}N$, ‰	N Meas., ppm	Spectral type	μT (1282), mm^{-1}	Platelet Pos., cm^{-1}	Platelet I(B')/μT	H3107 Pk Area	H3311 Pk Area	% Nitrogen in B form	Nitrogen, ppm	T(NA), °C
EC-01	YL	N-L							Ib-IaA	10.23	–	–	8.1	2.2	0 (9% Ib)	1769	847
EC-07	CL	»							IaA	8.42	–	–	4.3	–	<1	1355	≤1014
EC-02/2	PY	»							»	7.75	–	–	2.4	–	1016		
EC-32	CL	»	rou(sc), fr(old)	weak	–	*	*	*	»	7.20	–	–	16.8	2.9	<1	1158	≤1018
EC-12	PY	»							»	6.82	–	–	25.3	4.1	<1	1097	≤1019
EC-11	CL	»							»	6.71	–	–	10.5	1.6	<1	1079	≤1019
EC-14	»	»							»	6.34	–	–	0.8	–	<1	1021	≤1020
EC-06	PY	M	rou(agg), fr(new)	weak	–	–10.67	–4.6 ± 0.3	1617 ± 114	»	6.01	–	–	3.4	–	<1	967	≤1021
EC-13	CL	N-L							»	5.33	–	–	1.5	–	<1	857	≤1024
EC-31/3	PY	»							»	4.25	–	–	28.2	3.6	<1	684	≤1029
EC-17	CL	»	octa(dis), fr(old)	strong	+	–7.56	–2.4 ± 0.5	2290 ± 245	»	9.72	1363	0.01	18.5	2.8	<1	1576	≤1029
EC-31/1	PY	»							»	4.09	–	–	28.8	3.4	<1	657	≤1030
EC-31/2	»	»							»	3.98	–	–	28.1	4.1	<1	641	≤1030
EC-37	CL	»	octa(sc)	weak	–	*	*	*	»	2.47	–	–	1.0	–	<1	398	≤1040
EC-28	»	»							»	3.89	1367	0.09	0.1	–	2	631	1050
EC-24	»	»							IaAB(M)	5.48	1374	0.56	0.9	–	7	922	1071
EC-39	»	»							IaA	2.67	–	–	1.8	–	4	438	1073
EC-02/1	PY	»							»	0.68	–	–	1.3	–	2	110	1088
EC-21	CL	»							»	0.98	1364	0.39	0.0	–	4	161	1096
EC-34	»	»	octa(sc), fr(new)	strong	–	–6.36	–6.0 ± 1.2	818 ± 57	IaAB(M)	6.17	1373	2.47	2.3	–	25	1197	1098
EC-03	»	»							»	1.45	1366	0.69	0.8	–	8	246	1103
EC-19	»	»							»	2.85	1369	1.70	0.5	–	18	520	1107
EC-08/2	»	»							»	2.55	1370	1.91	0.9	–	19	471	1112

EC-40	»	»							»	4.34	1367	3.46	2.1	–	35	914	1115
EC-30	»	»							»	1.68	1370	1.36	0.6	–	15	299	1115
EC-15	»	»							»	1.02	1365	0.85	1.7	–	10	174	1116
EC-35	CL	»							IaAB(L)	6.18	1375	2.44	27.8	–	53	1600	1118
EC-30	GY	»							IaAB(M)	1.65	1366	1.83	0.6	–	20	305	1122
EC-27	»	»	macl + octa(agg)	weak	–	–9.00	–4.7 ± 1.2	1485 ± 104	»	4.57	1369	7.00	2.0	–	56	1217	1129
EC-09	PP	»							»	2.87	1367	5.19	0.9	–	44	668	1132
EC-10	GL	»							IaAB(L)	2.15	1370	2.82	0.0	–	39	471	1134
EC-25	»	»							IaAB(M)	1.07	1363	1.96	0.7	–	21	201	1135
EC-16	»	»	rou(sc), fr(new)	moderate	–	–9.43	+0.8 ± 1.4	437 ± 33	»	2.40	1365	4.90	1.1	–	52	602	1141
EC-29	»	»							»	1.30	1365	3.45	1.6	–	40	289	1148
EC-33	PB	»							»	0.52	1366	1.83	0.8	–	20	96	1151
EC-22	CL	»							IaAB(L)	0.68	1365	2.11	0.4	–	31	139	1156
EC-08	»	»							»	1.07	1367	4.79	2.1	–	57	289	1165
EC-36	»	»							IaAB(M)	0.73	1365	4.44	2.8	–	43	168	1165
EC-23	»	»							IaAB(L)	0.50	1370	3.06	0.4	–	41	111	1173
EC-38/2	»	»	octa(parallel agg)	moderate	+	–16.66	+2.9 ± 5.7	81 ± 10	»	0.38	1363	3.63	1.8	–	68	123	1199
EC-38/4	»	»	»	»	»				IaAB(K)	0.45	–	0.00	1,5	–	75	174	1199
EC-20	PB	»				–7.56	–9.4 ± 5.2	27 ± 6	IaAB(L)	0.24	1370	3.54	0,4	–	51	60	1199
EC0-26	CL	»							IaAB(M)	0.35	1365	14.25	2,0	–	74	119	1209
EC-18/2	»	»							IaAB(K)	0.10	1369	0.85	0,8	–	43	24	1215
EC-18/1	»	»							IaAB(L)	0.12	1368	1.79	0,6	–	50	30	1217
EC-04	»	U							IIa	–	–	–	0,0	–	–	<10	–
EC-05	PB	N-L	macl, fr(old)	strong	–	–7.67	–	<10	»	–	–	–	0,1	–	–	<10	–

***Sample lost during isotopic analysis. Color: CL — colorless, PB — pale brown, PY — pale yellow, YL —yellow, pp — pale pink, GY — gray. Resorption: N-L — none-low, M — moderate, U — unknown. External form: octa — octahedral, macl — macle, rou — rounded, sc — single crystal, agg — aggregate, fr — fracture. μT(1282) — total absorbance at 1282 cm^{-1} per mm diamond thickness, I(B')/μT — area of the platelet peak/μT(1282), H3107 and H3311 Pk Areas — area of the hydrogen defect peaks at 3107 and 3311 cm^{-1}, T(NA) — nitrogen aggregation temperature calculated for a mantle residence time of 1.65 Ma.**

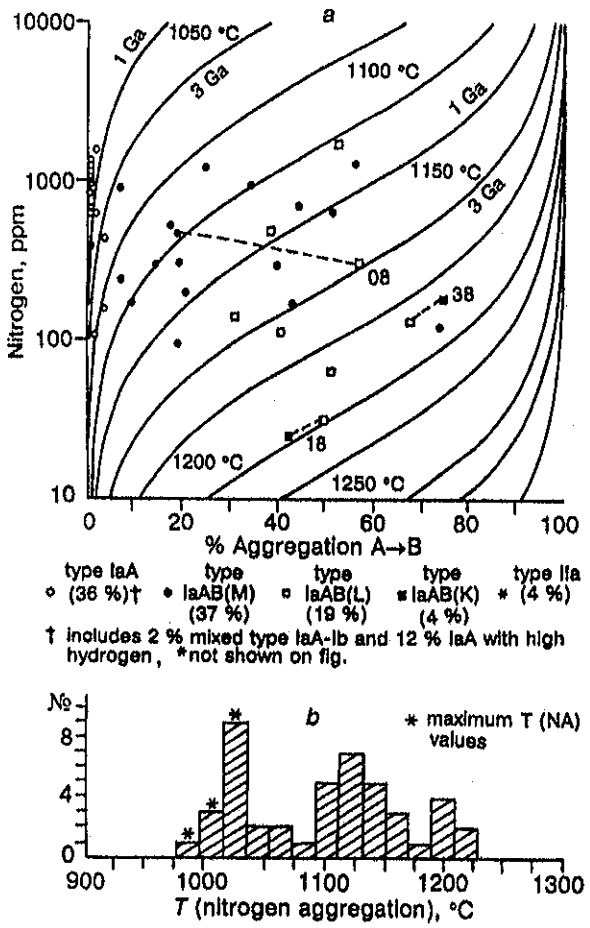

Fig. 8. Ector pipe diamonds, Northern territory, Australia. *a* — Nitrogen concentration; *b* — temperature histogram for t_{MR} = 1.65 Ga.

(iii) a population of high temperature diamonds (T(NA) ~1200 °C for a 1.65 Ga residence time), again with platelet intensities consistent with these temperatures (type-L and type-K behaviour). Type II, i.e. nitrogen free diamonds were not common in the microdiamonds studied (2 out of 40).

The nitrogen aggregation temperature, T(NA), for one yellow type 1b - 1aA microdiamond was calculated to be 847 °C if a mantle residence time of 1.65 Ga is assumed. This suggests that diamonds of this type in the Merlin kimberlite have had a much shorter residence time in the mantle than 1.65 Ga and perhaps have an age much closer to the kimberlite eruption age.

An unusual feature of some of the microdiamonds is the exceptionally high level of hydrogen. This is revealed in the IR spectra (Fig. 9). The high hydrogen levels are usually in diamonds with low levels of nitrogen aggregation.

Carbon and nitrogen isotope measurements were made for eight microdiamonds from the Ector pipe. The ^{13}C signature is lighter than that for average peridotitic diamonds worldwide (Fig. 10).

The temperature histogram (Fig. 8), the variety of microdiamond morphologies and the major deviation from a normal size distribution at 0.2 mm (Fig. 7) all suggest that several populations of diamonds are present in the Merlin kimberlites.

CONCLUSIONS

The Merlin kimberlites are predominantly diatreme facies kimberlites with some hypabyssal material present at depth. They are geochemically similar to the Aries kimberlite and the Bow Hill lamprophyres in Western Australia. The kimberlites contain lherzolitic and harzburgitic rocks from a deep mantle source

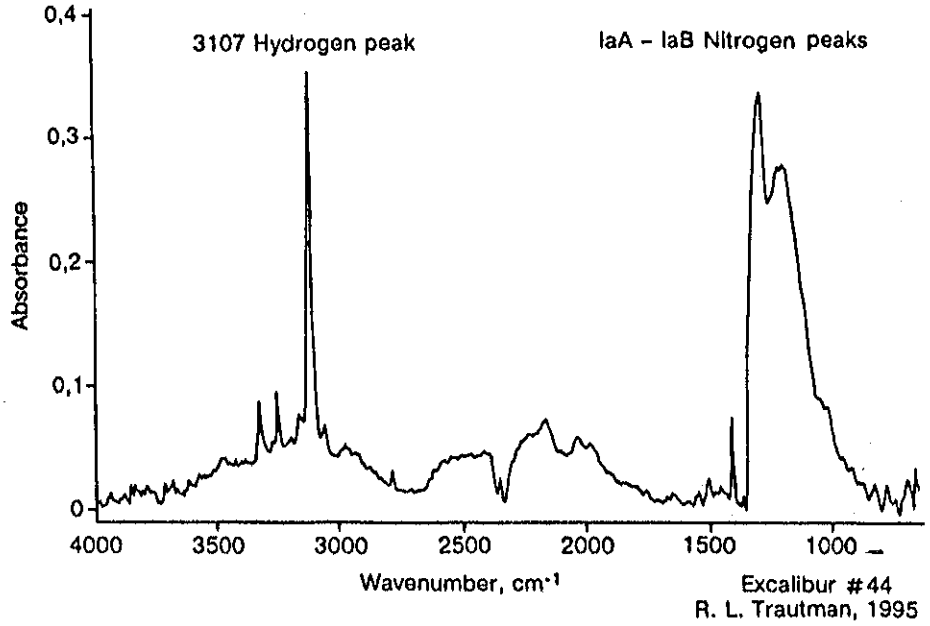

Fig. 9. FTIR spectrum of a Merlin microdiamond with an extreme 3107 hydrogen intensity.

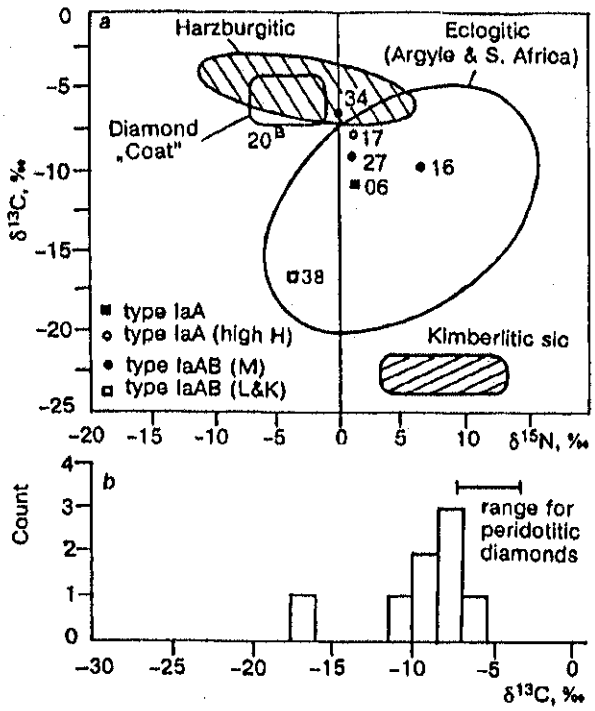

Fig. 10. a — $\delta^{13}C$ vs $\delta^{15}N$ diagram showing isotopic composition of diamonds from the Ector pipe in relation to the low $\delta^{13}C$ and the high $\delta^{15}N$ fields for octahedral diamonds from Argyle, Arkansas and various South African pipes; the field of diamond "coat" (Boyd and Pillinger, 1994); and the isotopic composition of SiC (moissanite) from the Aikhal kimberlite (Marthez et al., 1995). The Ector diamonds have $\delta^{13}C$ compositions that are generally lighter than peridotitic diamonds from worldwide sources and have $\delta^{15}N$ composition that are intermediate between the low and high $\delta^{13}C$ groups suggesting the C and N in the Ector diamonds originated by mixing between two distinct resevoirs: a mantle component and a recycled crustal or SiC-derived component. There are no obvious correlations between $\delta^{13}C$, $\delta^{15}N$ and IR spectral type of the diamonds. One type IIa diamond (<10 ppm N), not able to be shown in "a", has a $\delta^{13}C$ isotopic composition of –7.7%. b — $\delta^{13}C$ histogram.

region and appear to contain several populations of diamonds. Further studies are required to confirm the diverse nature of the diamonds.

ACKNOWLEDGMENTS

This study was supported by Ashton Mining Limited and the Australian Diamond Exploration Joint Venture, and their permission to publish is gratefully acknowledged. Joneen Lemon is thanked for her assistance in preparing the text and diagrams.

REFERENCES

[1] B. A. Pietsch, D. J. Rawlings, P. M. Creaser, P. D. Kruse, M. Ahmad, P. A. Ferenczi, and T.L.R. Findhammer, *Bauhinia Downs Explanatory Notes*, Department of Mines and Energy, Northern Territory Geological Survey.

[2] C. R. Clement, E. M. W. Skinner, and B. H. Scott Smith, Kimberlite redefined, *J. Geol.*, 32, p. 223, 1984.

[3] R. H. Mitchell, *Kimberlites: Mineralogy, geochemistry and petrology*, Plenum Publishing, New York, 1986.

[4] A. R. Woolley, S. C. Bergman, A. D. Edgar, M. J. Le Bas, R. H. Mitchell, N. M. S. Rock, and B.H. Scott Smith, *Classification of the lamprophyres, lamproites, kimberlites and the kalsilite-, melilite- and leucite-bearing rocks. (Recommendations of the IUGS subcommission on the systematics of igneous rocks)*, Canadian Mineralogist, in press.

[5] E. M. W. Skinner and C. R. Clement, Mineralogical classification of South Africa kimberlite, in: *Proc. 2nd International Kimberlite Conference, vol. 1, Kimberlites, Diatremes and Diamonds: Their Geology, Petrology and Geochemsitry, F. R. Boyd and H. O. A. Meyer (eds.)*, American Geophysics Union, Washington, p. 129, 1979.

[6] B. H. Scott Smith, E. M. W. Skinner, and C. R. Clement, Further data on the occurrence of pectolite in kimberlite, *Mineral. Mag.*, 47, p. 75, 1983.

[7] J. B. Hawthorne, Model of a kimberlite pipe, *Physics and Chemistry of the Earth*, 9, p. 1, 1975.

[8] C. R. Clement, *A comparative geological study of some major kimberlite pipes in the northern Cape and Orange Free State*, Unpublished Ph. D. thesis, University of Cape Town, South Africa, 1992.

[9] C. R. Clement and E. M. W. Skinner, A textural-genetic classification of kimberlites, *Trans. Geol. Soc. South Africa*, 88, p. 403, 1985.

[10] C. R. Clement and A. M. Reid, *The origin of kimberlite pipes: An interpretation based on a synthesis of geological feautres, displayed by Southern African occurrences in Kimberlites and Related Rocks, J. Ross (ed.)*, Geological Society of Australia, Special Publication, 14, 1, p. 632, 1989.

[11] N. G. Ware, Computer programs and calibration with the PIBS technique for quantitative electron probe analysis using a lithium-drifted silicon detector, *Computers and Geosciences*, vol. 7, p. 167, 1981.

[12] W. R. Taylor, L. A. Tompkins, and S. E. Haggerty, Comparative geochemistry of West African kimberites: evidence for a micaceous kimberlite endmember of sublithospheric origin, *Geochim. Cosmochim. Acta*, 58, p. 4017, 1994.

[13] D. C. Fielding and A. L. Jacques, Geology, petrology and geochemistry of the Bow Hill lamprophyre dykes, Western Australia, in: *4th Internation. Kimberlite Conference Proceedings*, vol. 1, p. 206, 1989.

[14] C. B. Smith, H. Lucas, A. E. Hall, and R. R. Ramsay, in: H. O. A. Meyer and O.H. Leonards (eds.), *Diamonds: Characterisation, Genesis and Exploration*, CPRM, Brazil, p. 312, 1994.

[15] H. O. A. Meyer, Inclusions in diamond, in: P. H. Nixon (ed.), *Mantle Xenoliths*, Wiley and Sons, England, p. 501, 1987.

[16] N. V. Sobolev, *Deep-seated inclusions in kimberlites and the problem of the composition of the upper mantle*, Nauka, Novosibirsk, 1974.

29 August 1996

ISSN 1068-7971

RUSSIAN GEOLOGY AND GEOPHYSICS

ГЕОЛОГИЯ И ГЕОФИЗИКА

1

Vol. 38, 1997

Special Issue:

Proceedings of the Sixth International Kimberlite Conference

Vol. 1: Kimberlites, Related Rocks and Mantle Xenoliths

Allerton Press, Inc. / New York

CONTENTS

VOLUME 38 NUMBER 1 1997

RUSSIAN GEOLOGY AND GEOPHYSICS

PROCEEDINGS OF THE SIXTH INTERNATIONAL KIMBERLITE CONFERENCE

VOLUME 1. KIMBERLITES, RELATED ROCKS AND MANTLE XENOLITHS

	PAGES RUSSIAN	PAGES ENGLISH
Dedication	1	i
Preface	7	3
Kimberlites in the Slave craton, Northwest Territories, Canada: a preliminary review. J.A. Pell	9	5
Diamond-bearing volcaniclastic kimberlites in Cretaceous marine sediments, Saskatchewan, Canada. P. H. Nixon and K. Leahy	19	17
The geology of the Orapa A/K1 kimberlite Botswana: further insight into the emplacement of kimberlite pipes. M. Field, J. G. Gibson, T. A. Wilkes, J. Gababotse, and P. Khutjwe	25	24
Volcanology of the carbonatitic Gross Brukkaros volcanic field, Namibia. V. Lorenz, S. Kurszlaukis, T. Stachel, and I. G. Stanistreet	42	40
Phase petrology, geochemistry and evolution of the ultrabasic-carbonatitic Blue Hills complex (*Southern Namibia*). S. Kurszlaukis and L. Franz	51	50
Ultrabasic potassic low-volume magmatism and continental rifting in North-Central Tanzania: association with enhanced heat flow. J. B. Dawson, D. James, C. Paslick, and A. M. Halliday	67	69
The Merlin kimberlites, Northern Territory, Australia. D. C. Lee, H. J. Milledge, T. H. Reddicliffe, B. H. Scott Smith, W. R. Taylor, and L. M. Ward	78	82
Shrimp U-Pb ages of perovskite from Yakutian kimberlites. P. D. Kinny, B. J. Griffin, L. M. Heaman, F. F. Brakhfogel, and Z. V. Spetsius	91	97
Laser $^{40}Ar/^{39}Ar$ dating of phlogopites from Southern African and Siberian kimberlites and their xenoliths: constraints on eruption ages, melt degassing and mantle volatile compositions. D. G. Pearson, S. P. Kelley, N. P. Pokhilenko and F. R. Boyd	100	106
Low-titanium Aldan lamproites (Siberia): melt inclusions in minerals. L. I. Panina	112	118
Geochemistry and genesis of lamproites of the Aldan Shield. N. V. Vladykin	123	128
Evolution of lamproites suggested by melt inclusions in minerals. V. V. Sharygin	136	142
New data on cocites, ultrapotassic basic rocks in North Vietnam. G. V. Polyakov, Nguyen Trong Yem, P. A. Balykin, Tran Trong Hoa, L. I. Panina, Ngo Thi Phuong, Hoang Huu Thanh, Chan Quoc Hung, V. V. Sharygin, Bui An Nien, Vu Van Van, Hoang Viet Hang	148	154

(continued)

	PAGES RUSSIAN/ENGLISH	
Garnet peridotites from the Tres Ranchos IV kimberlitic pipe, Alto Paranaiba igneous province, Brazil: geothermobarometric constraints. J. B. Carvalho and O. H. Leonardos	159	168
Mantle metasomatism and melting in mantle-derived xenoliths from the Udachnaya kimberlite; their possible relationship with diamond and kimberlite formation. L. V. Solovjeva, K. N. Egorov, M. E. Markova, A. D. Kharkiv, K. E. Popolitov, and V. G. Barankevich	172	182
Geochemical characteristics of mantle xenoliths from the Udachnaya kimberlite pipe. N. Shimizu, N. P. Pokhilenko, F. R. Boyd and D. G. Pearson	194	205
A unique metasomatized peridotite xenolith from the Mir kimberlite, Siberian Platform. V. N. Sobolev, L. A. Taylor, G. A. Snyder, N. V. Sobolev, N. P. Pokhilenko, and A. D. Kharkiv	206	218
The meaning of Sm/Nd apparent ages from kimberlite-derived, coarse grained low temperature garnet peridotites from Yakutia. M. Günther and E. Jagoutz	216	229
Trace elements in minerals from eclogites from the Udachnaya kimberlite pipe, Yakutia. Z. V. Spetsius and W. L. Griffin	226	240
Detailed petrology and geochemistry of a rare corundum eclogite xenolith from Obnazhennaya, Yakutia. Qu Qi, L. A. Taylor, G. A. Snyder, R. N. Clayton, T. K. Mayeda, and N. V. Sobolev	223	247
Metasomatic reequilibration of mantle xenoliths from the Gibeon kimberlite province (*Namibia*). L. Franz, G. P. Brey, and M. Okrusch	245	261
Thermobarometry and reconstructed chemical compositions of spinel-pyroxene symplectites: evidence for pre-existing garnet in lherzolite xenoliths from Czech Neogene lavas. L.G. Medaris, Jr., J.H. Fournelle, H.F. Wang, and E. Jelinek	260	277
Water in the Earth's mantle. G. Dreibus, E. Jagoutz, and H. Wänke	269	287
Volatile components in the upper mantle (*from data on fluid inclusions*). A. A. Tomilenko, A. I. Chepurov, Yu. N. Pal'yanov, L. N. Pokhilenko, and A. P. Shebanin	276	294